



Multi-compartment tumor organoids

Meng-Horng Lee ^{1,2,†}, Gabriella C. Russo ^{1,2,†}, Yohan Suryo Rahmanto ³, Wenxuan Du ^{1,2}, Ashleigh J. Crawford ^{1,2}, Pei-Hsun Wu ^{1,2}, Daniele Gilkes ^{1,2,3}, Ashley Kiemen ^{1,2}, Tsutomu Miyamoto ³, Yu Yu ^{3,4}, Mehran Habibi ⁵, Ie-Ming Shih ^{3,4}, Tian-Li Wang ^{3,4}, Denis Wirtz ^{1,2,3,*}

Organoid cultures are widely used for tumor modeling because they preserve many phenotypic features of cancer cells *in vivo*. However, current organoids present issues of consistency, efficiency, mimicry, and cell-seeding control. More importantly, they can only contain only one extracellular matrix (ECM) compartment at a time, while solid tumors feature two main ECM compartments: the basement membrane and the stromal matrix. Here, we develop, test, and validate a high-throughput oil-in-water droplet microtechnology to generate highly uniform, small-volume, multi-compartment organoids. Each organoid culture features microenvironmental architectures that mimic both the basement membrane and stromal barriers. This matrix architecture, which allows us to simultaneously take into account and assess the proliferative and invasive properties of cancer cells in a single platform, has profound effect on observed drug responsiveness and tumor progression that correlate well with *in vivo* and clinical outcomes. Our method was tested on multiple types of cells including primary breast and ovarian cancer cells and immortalized cell lines, and we determined our platform is suitable even for cancer cells of poor standard organoid-forming ability such as primary patient samples. These new organoids also allow for direct orthotopic mouse implantation of cancer cells with unprecedented success.

Keywords: 3D model; Tumor microenvironment; Primary cancer cell culture; Tumor progression; Biomaterials

Introduction

Tumor organoids are widely used to maintain and study cancer cells isolated from patients [1-8]. Organoids have been used to identify molecular pathways that drive tumor progression [9-13] discover potential cancer biomarkers [14-19] and predict patient response to customized pharmacological treatments

¹ Johns Hopkins Physical Sciences - Oncology Center and Johns Hopkins Cancer Cell Biology Imaging Research Center, The Johns Hopkins University, Baltimore, MD 21218, USA

²Department of Chemical and Biomolecular Engineering, The Johns Hopkins University, Baltimore, MD 21218, USA

³ Departments of Pathology and Oncology and Sydney Kimmel Comprehensive Cancer Center, The Johns Hopkins School of Medicine, Baltimore, MD 21205,

⁴ Department of Gynecology and Obstetrics, Johns Hopkins Medical Institutions, Baltimore, MD 21287, USA

⁵ Department of Surgery, The Johns Hopkins School of Medicine, Baltimore, MD 21205, USA

st Corresponding author.

E-mail address: Wirtz, D. (wirtz@jhu.edu)

[†] These authors contributed equally.

[1,7,8,20-22]. However, before the implementation of organoids at scale for reliable application in high-throughput drug screening and predictive modeling *ex vivo*, greatly enhanced consistency, efficiency, mimicry, and cell-seeding control are imperative [10,23-27].

Here, we introduce a novel oil-in-water droplet microtechnology to produce a highly consistent, small-volume organoids culturing platform. Each organoid culture requires 1 μ l of Matrigel instead of typically >50 μ l Matrigel per conventional organoid culture. Hence, for the same amount of tumor tissue, many more individual organoids can be simultaneously created. Unlike standard organoid culture, this efficient platform avoids having to move organoids/cells out of the original 3D extracellular matrix (ECM) and transfer them to multi-well assay plates before drug testing/screening applications, which greatly reduces organoid-to-organoid variability [1,8,22].

Moreover, current organoid cultures are limited to the use of only one ECM component at a time, typically either Matrigel or collagen I. This is a major issue as cells in tumor organoids mostly grow and invade/migrate little in Matrigel, while cells mostly invade and grow little in collagen I [28-32] (see also below). In other words, proliferation and invasion, two key drivers of malignancy, cannot be fully included simultaneously in conventional organoid cultures. Our new organoids feature a two-compartment architecture composed of juxtaposed recombinant basement membrane (rBM) and main stromal protein collagen I. These new organoids allow us to study highly invasive cancer cells, which are notoriously difficult to encapsulate [33,34]. We demonstrate the predictive power of these new organoids in recapitulating tumor progression in vivo and drug responsiveness in patients. We also provide an additional application of our methodology: to successfully initiate tumor xenografts with cells that are notoriously difficult to enhance tumorigenicity.

Results

Control of organoid volume, matrix architecture, and tumor cell growth

Following the initial steps of pro-oncogenic transformation, growing carcinoma tumor cells are first confined by a basement membrane rich in extracellular-matrix (ECM) components laminin, collagen IV, nidogen, and heparan proteoglycans [35]. Then, through disruption of this basement membrane and via a switch from a proliferative to an invasive phenotype, tumor cells spread into the surrounding stromal matrix, which is rich in collagen I [36,37]. To mimic this complex two-compartment ECM architecture, we have developed a novel oil-in-water droplet microtechnology that reliably and rapidly generates cultures of small organoids made of two matrix compartments (Fig. 1a): a core made of rBM (reconstituted basement membrane) Matrigel impregnated with cancer cells and an outer layer made of collagen I.

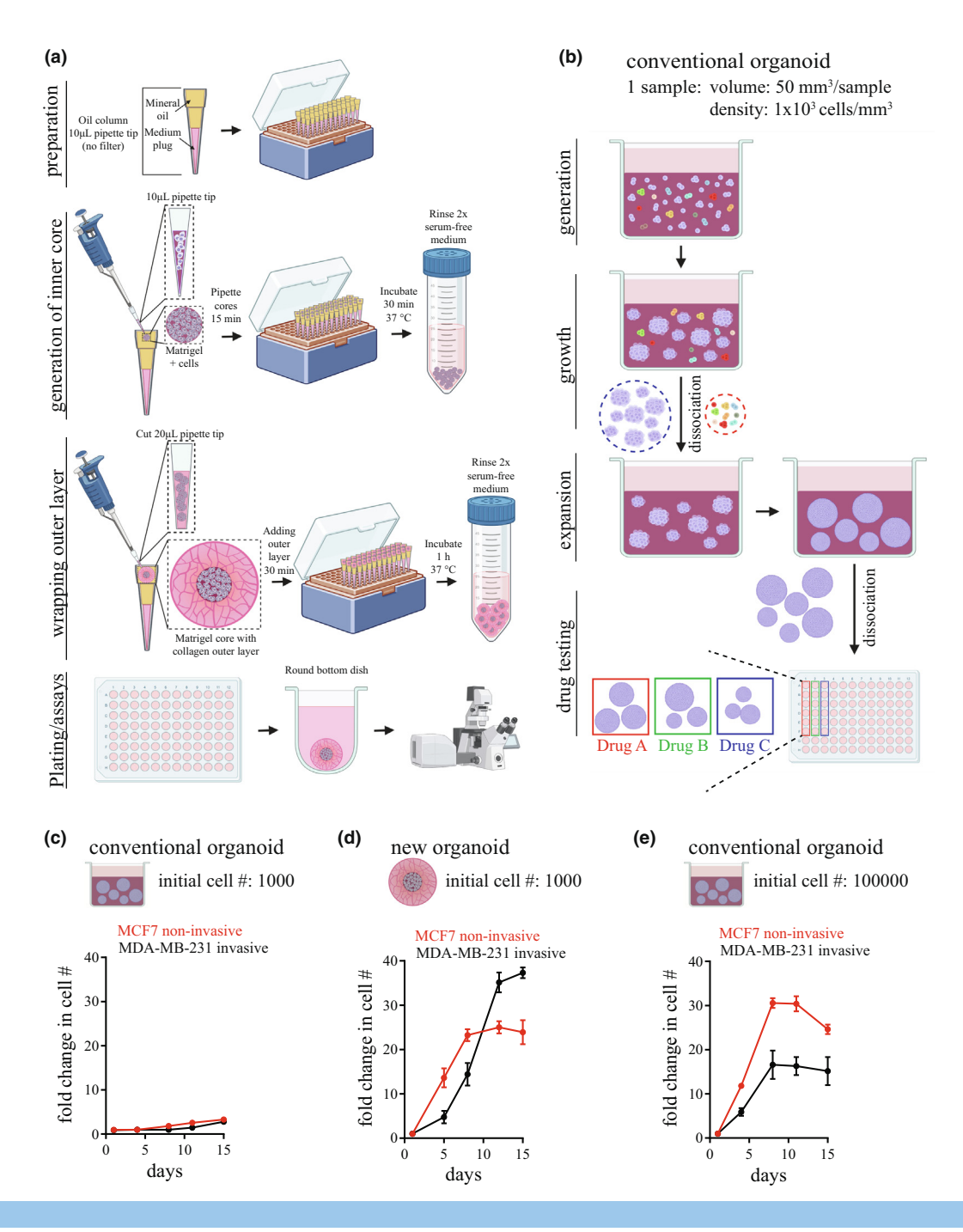
A controlled number of cancer cells is mixed with the first extracellular-matrix material (here Matrigel) and then pipetted into an oil column filled with approximately 80 μ L of mineral oil. The surface tension between water and oil and the resulting Plateau-Rayleigh instability molds the matrix into uniform

spherical droplets. To add a second ECM compartment, we harvest the gelled droplets, which will become the inner cores, using a modified pipette tip and placing them into warm serum-free medium to remove the mineral oil. To ensure complete removal of the oil, we rinse twice and move to a fresh conical tube prior to wash 2. We then prepare the collagen gel solution for the outer layer, using a protocol that allows us to easily tune the collagen concentration (FRALEY). Utilizing modified pipette tips, we mix the droplets into the second ECM (e.g. collagen I) and generate a well-mixed solution. We then place the solid inner core and liquid second layer into a column filled with approximately 80 μL of mineral oil (Fig. 1a). After a second incubation step to allow for the second layer to gel, we again rinse the now twocompartment organoids in warm serum-free medium to remove all mineral oil prior to plating them in a round-bottom 96-well plate. Compartments composed of other ECM materials and cells can be added by simply repeating this process.

Below, we first present an organoid model in which cancer cells are enclosed inside an inner compartment composed of rBM Matrigel (3 mg/mL) and an outer compartment of stromal ECM type I collagen (2 mg/mL) and highlight how this more physiological architecture affects fundamentally tumor cell proliferation, invasion, and drug responsiveness compared to standard Matrigel-only and collagen-only organoids (Fig. 1b). In the following sections, we show how we can integrate stromal cells (immune cells) in the collagen I outer later in a co-cultured two-compartment organoids, further improving upon physiological relevance of the model.

Our organoid cultures require a lot less ECM material per organoid than traditional organoid cultures (Fig. 1a). Our ability to generate 1 µL Matrigel droplets mixed with cancer cells allowed us to equally distribute cells into 50 individual cultures instead of one larger organoid when using the conventional approach, which uses 50 times more Matrigel to generate one organoid dome (Fig. 1b). Since these two-compartment organoids are dispensed into individual oil columns (i.e. one organoid per column), organoids do not have to be disturbed and removed from the original 3D matrix for cell expansion, as typically required for conventional organoid cultures (Fig. 1b). Our method has a high success rate in generating uniform spheres containing a desired cell density. The main challenge in producing double-layered organoids is the addition of the second ECM layer. This is because either multiple cores are picked up unintentionally or cores dissociate from the second layer if mineral oil is not completely removed prior to the "wrapping outer layer" step. Finally, cores containing air bubbles can be lost during the washing steps, and therefore, it is important to gently mix cells and Matrigel to prevent bubbles.

Our oil-in-water microtechnology produces more uniform organoids than conventional organoids. Having precise control over the seeding cell density is important because the density of cancer cells in 3D culture settings can influence their phenotype and their ability to migrate and invade [29,30]. For the same nominal seeding density, the measured coefficient of variation in cell numbers in the new organoids was <20% according to PrestoBlue viability reading (Supplementary Fig. 1a). In contrast, if organoids were isolated from the 3D ECM and placed in multiple assay wells, the coefficient of variation in cell number among



Oil-in-water droplet technology to make uniform, small-volume, two-compartment organoids. (a) Schematics for the generation of novel two compartment model utilizing oil-in-water droplet technology to layer two biomaterials together in a precise and controlled manner. Oil columns are generated from unfiltered 10 µl pipette tips by first aspirating medium to create a "plug" at the bottom. This allows us to fill the top of the pipette tip with mineral oil. Matrigel inner cores are generated by mixing a desired number of cancer cells with a controlled volume of Matrigel at a concentration of 3 mg/mL. The cores incubate for 30 min at 37 °C. Once gelled, cores are rinsed to remove all mineral oil prior to wrapping with the second ECM layer, collagen I gel at 2 mg/mL. The two-compartment organoid is incubated for 1 h at 37 °C. The two-compartment organoids are then washed again to remove all mineral oil prior to plating. (b) Design and manufacture of traditional organoid culture using Matrigel only. (c and d) Growth rates of cancer cells in conventional organoids with different initial cell seeding numbers in Matrigel. (e) Growth rates of cancer cells in two-compartment organoids. Cells used in panels c and d are MCF7 (red curves) and MDA-MB-231 breast cancer cells (black curves). In panels (c and d), each curve encompasses three biological repeats and each repeat has five replicates for a total of 15 tested organoids.

wells was >80% because dissociated organoids have different sizes and contain different numbers of cells (Supplementary Fig. 1b-d).

To demonstrate the precision in generating cores and organoids of a specific size (here a 1 μL drop for the core and a

 $10~\mu L$ total volume with second layer), we calculated the coefficient of variation of inner and outer volume measurements on day 1 (Supplementary Fig. 1e). Both the inner and outer radius measurements have a coefficient of variation under 10%. To demonstrate the accuracy of PrestoBlue as a measure of growth

differences, we correlated the raw reading of PrestoBlue (RFU) to measured protein concentration of six different cell lines (Supplemental Fig. 1f). The resulting R squared value was 0.85, demonstrating a strong correlation between PrestoBlue output and total cell content in the organoid system. Further justification of PrestoBlue as a way to track organoid growth and proliferation is described in the methods section and Supplementary Fig. 5a.

The growth of cells can readily be optimized. Thanks to the small volume of the inner Matrigel compartment, we can create organoid cultures of highly controlled nominal cell density. By adjusting the seeding cell density, the growth of cancer cells in our organoid cultures can be readily optimized (Supplementary Fig. 1g,h). In our novel organoid culture, cancer cells can successfully propagate even when the initial seeding cell number is very low (<1000 cells), which is nearly impossible to achieve using the conventional organoid culture method (Fig. 1c and d). Moreover, invasive MDA-MB-231 breast cancer cells in conventional organoid cultures grew much more slowly than non-invasive MCF7 breast cancer cells (Fig. 1e). In contrast and similarly to the in vivo case [38], invasive cells incorporated into the twocompartment organoids could grow more than non-invasive cells (Fig. 1d). This is partly because the outer collagen compartment in the new organoid culture supported effective cancer cell invasion, as measured by tracking the volume of the inner and outer compartments (Supplementary Fig. 1i,j).

Justification for a two-compartment matrix architecture

The primary tumor microenvironment is complex and composed of different ECM molecules and compartments as well as cell types, including immune cells and cancer-associated fibroblasts, which modulate tumor progression and drug responsiveness [39,40]. Thus, the fact that our organoids can incorporate at least two different types of ECM compartments and can include different types of cells in these compartments enhances the physiological relevance of our organoid culture method.

To determine the effects of the proper organization of the ECM architecture on tumor-cell growth and invasion, we generated four ECM architectures (Fig. 2a). In addition to the configuration presented in Fig. 1 (Matrigel core and collagen outer layer), we produced three other organoids with (i) Matrigel only, i.e. the two compartments were made of Matrigel, which is similar to a standard organoid made of Matrigel, (ii) a collagen core with a Matrigel outer layer, and (iii) collagen only, i.e. the two compartments were made of collagen, which is similar to a standard organoid made of Collagen I. Given the known properties of these two ECM materials, we anticipated that cells would primarily proliferate in Matrigel-only organoids and would primarily invade in collagen-only organoids. In organoids with reversed ECM layers - collagen in the core and Matrigel in the outer layer - we anticipated that cells would remain confined to the inner collagen compartment as they cannot migrate into Matrigel [41].

As anticipated [39], we found that cancer cells in organoids with a Matrigel core formed larger tumors than in organoids with a collagen core, confirming that the type of ECM impacts tumor size (Fig. 2b). Tumor cells in Matrigel grew more rapidly than the cells in collagen I, independent of the composition of the outer compartment, as anticipated from the known pro-proliferative

properties of Matrigel (Fig. 2c) [41,42]. Cancer cells invaded the outer compartment as singlets and small aggregates only when that compartment was collagen I (Fig. 2a). Tumors showed the fastest growth and invasion, measured by computing the volumetric ratio of the inner sphere to the outer sphere, when the inner compartment was Matrigel and the outer compartment was collagen I (Fig. 2d). The use of only one type of ECM material, which is the ECM architecture of standard organoids, significantly slowed down the impact of cell invasion and migration on the remodeling of the collagen I in the outer layer (Fig. 2e). The reverse (non-physiological) architecture of an inner collagen core containing cancer cells and an outer Matrigel compartment inhibited the invasion of cancer cells (Fig. 2a, d and e). The entirety of the outer collagen matrix was overtaken by highly invasive MD-MB-231 cancer cells and reorganized the matrix (Fig. 2a).

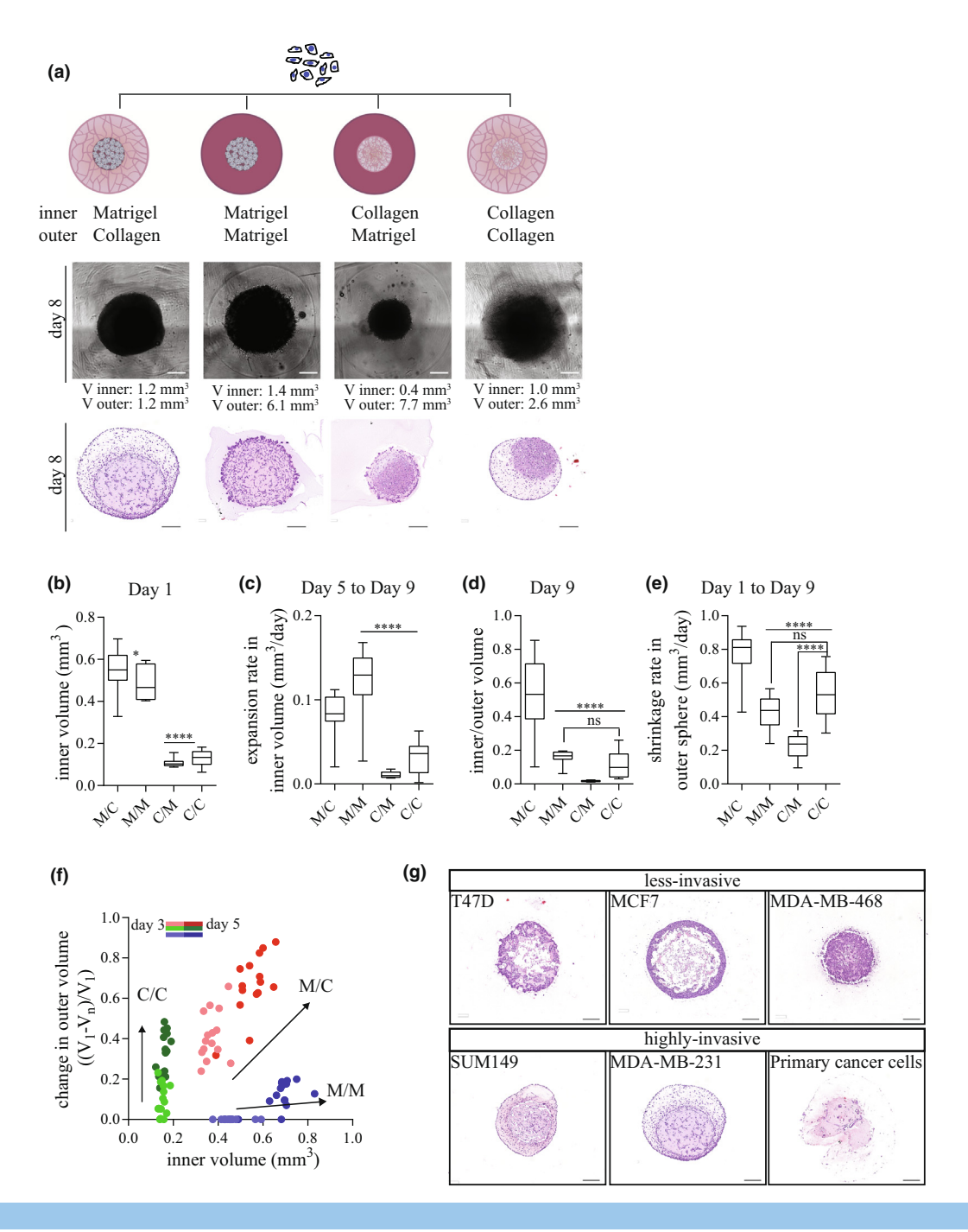
Our results support that our proposed system – a Matrigel core and a collagen outer layer- behaved most similarly to tumor progression observed *in vivo*: Cancer cells grow first in an environment confined by the basement membrane, traverse the boundary, and then migrate toward the collagen-rich matrix and remodel the tumor microenvironment. In sum, our new multicompartment ECM system allows us to study two key hallmarks of cancer progression- proliferation and invasion- at once, which is not achievable in single-biomaterial organoid models, demonstrated by correlating the change in inner volume with the change in outer volume (Fig. 2f).

All the above demonstrations were first conducted with commonly used MDA-MB-231 triple negative breast cancer cells. We successfully repeated these experiments with SUM149 inflammatory breast cancer cells and HCC1954 breast cancer cells, (an epithelial breast cancer cell line isolated from a primary stage IIA, grade 3 invasive ductal carcinoma with no lymph node metastases) (Supplementary Fig. 2a,b). Both cell lines demonstrated the same trend as observed in MDA-MB-231 cells: the Matrigel inner compartment with a collagen outer layer organoids showed the fastest organoid growth and onset of invasion (Supplementary Fig. 2a,b).

Together, these results indicate that the properly juxtaposed organization of the basement membrane-like compartment as the core and collagen I compartment at the outer layer made possible by our new organoids greatly impacts the growth and invasive properties of carcinoma cells. For a Matrigel/collagen bilayered architecture, cancer cells in the new organoids can progress via proliferation, invasion and remodeling of the surrounding ECM. Depending on the type of cancer cells used and associated cell–ECM and cell–cell interactions controlled by the modulable architecture of these new organoids, cells showed unique ways to organize themselves and the ECM (Fig. 2g).

Pre-clinical applications of two-compartment organoids

Next, we show that drug responsiveness of cancer cells in our new culturing platform correlates well with predicted clinical drug response. Clinical investigations have shown that patients with tumors featuring a high estrogen receptor alpha (ER) expression are associated with better response to hormone therapy and poorer response to cytotoxic chemotherapy [43–45]. To study the potential clinical translation of our two-compartment orga-



Differential progression of tumor cells using different configurations of matrix compartments. (a) Representative phase-contrast images and H&E images of two-compartment organoids containing MDA-MB-231 breast cancer cells after 7 days in culture. (b) Effect of ECM compartment composition for the growth of two-compartment organoids. Thanks to our oil-in-water droplet technology, the effect of the matrix composition of the inner core and outer compartment on drug responsiveness of cells could be examined. Bar graphs represent the mean ± SEM of the core volume of two-compartment organoids at day 1, (c) their growth between days 5 and 9 in culture, (d) their progression measured by the ratio of the volumes of the inner and outer compartments at day 9 in culture, and (e) the shrinking rate of the outer compartment of new organoids in four different configurations of the two matrix compartments. The core and outer compartments either contain Matrigel (M) and/or collagen I (C) (***** p < 0.001). Note that C/C and M/M configurations are two-compartment organoids where inner and outer compartments are both made of collagen or both made of Matrigel, respectively, which are equivalent to conventional organoids composed of a single compartment made of either collagen or Matrigel only. In panels (b–e), parameters for each organoids configuration encompasses three biological repeats and each repeat has five replicates for a total of 15 tested organoids. (f) Shrinkage of the outer compartment and expansion of the core tumor compartment of new organoids between days 3 and 5. Each datapoint corresponds to the volumes of the inner and outer compartments of an organoid measured at day 3 (light color) and day 5 (dark color). (g) Different patterns of tissue organization and invasion of new organoids composed of different types of cancer cells (cell lines and primary breast cancer cells) and cultured for a week, as assessed by sectioning followed by H&E staining and imaging. Scale bar, 200 mm.

noid model, we subjected organoids containing MCF7 ER+ breast cancer cells and MDA-MB-231 triple-negative breast cancer cells in their cores to estrogen receptor modulator Tamoxifen. Based on clinical observations, MCF7 organoids should respond well to Tamoxifen, as MCF7 cells express the estrogen receptor targeted by this drug. Tamoxifen should not impact the growth of

MDA-MB-231 organoids, as these cells do not have estrogen receptor. To compare our novel model to traditional organoids, we allowed the cells to grow for 8 days prior to drug treatment, which was given for 1 week before cell numbers in the organoids were assessed (Fig. 3a,f). When cultured in our novel two-compartment model, ER+ MCF7 organoids responded to low

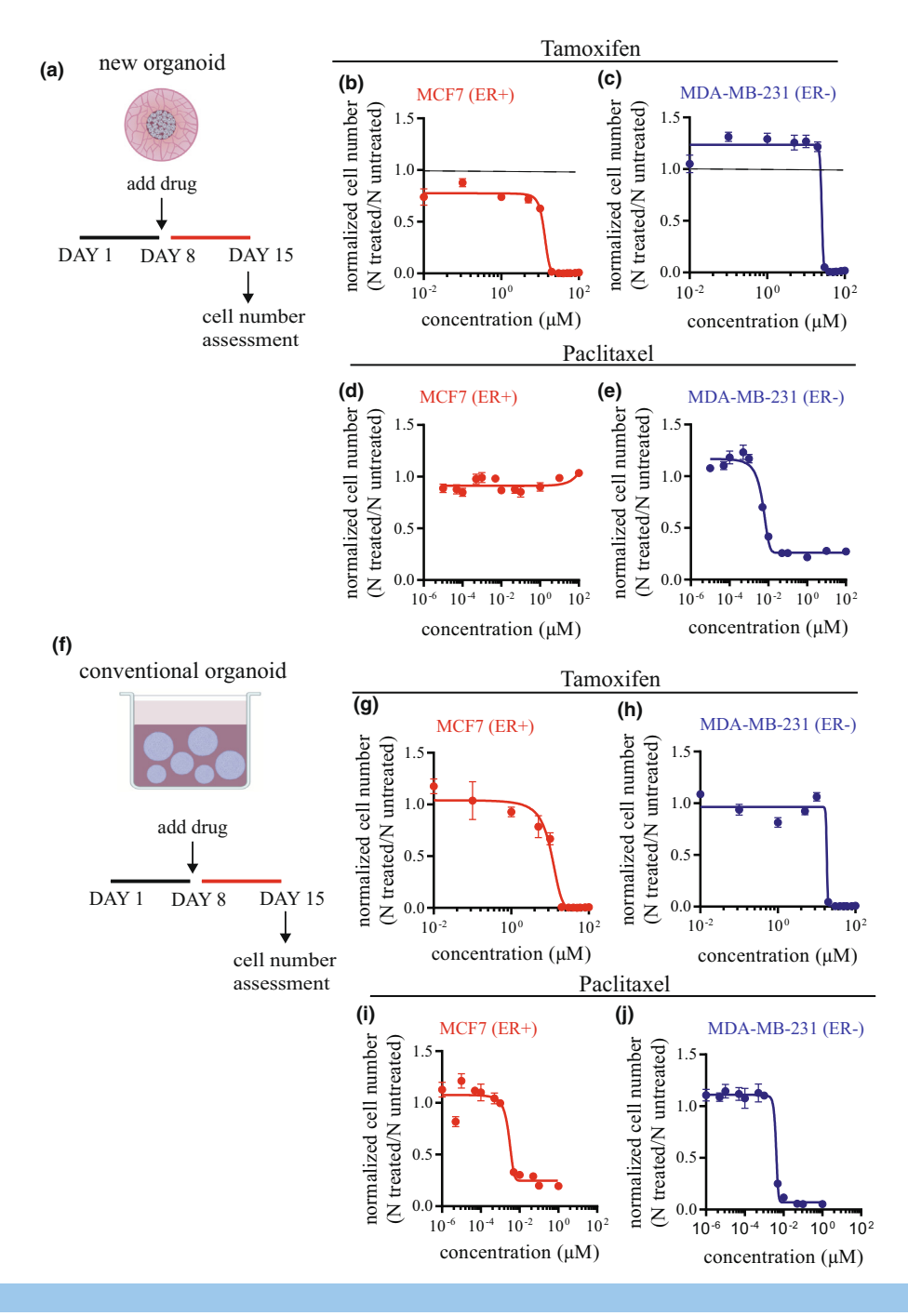


FIGURE 3

Drug responsiveness of conventional and two-compartment tumor organoids. (a–j) Two-compartment organoids and conventional organoids containing estrogen receptor-positive (ER+) MCF7 cells or ER⁻ MDA-MB-231 breast cancer cells and treated with ER modulator tamoxifen or cytotoxic drug paclitaxel. Responsiveness of MCF7 breast cancer cells (b, d, g and i) and MDA-MB-231 breast cancer cells (c, e, h and j) incorporated into the Matrigel core of (b–e) two-compartment organoids and (g–j) conventional organoids to (b, c, g and h) tamoxifen and (d, e, i and j) paclitaxel. For the two-compartment organoids, the outer compartment is made of collagen I. Drug doses are indicated in the panels. Each measurement in panels (b–e and g–j) encompasses three biological repeats and each repeat, and each repeat has five replicates for a total of 15 tested organoids.

dose of Tamoxifen, as anticipated based on clinical observations and ER— MDA-MB-231 organoids did not respond (Fig. 3b and c). In contrast, the same cells grown using conventional organoids predicted erroneously the same response for ER⁺ and ER⁻ cells to Tamoxifen treatment (Fig. 3g and h).

To test the predictive power of our new organoids to cytotoxic agents, we employed chemotherapeutic drug Paclitaxel. Based on clinical observations, ER+ MCF7 organoids should not respond to this cytotoxic drug whereas ER- MDA-MB-231 organoids should show response to treatment, as cytotoxic treatments are the most successful therapies for treatment of TNBC tumors [43-45]. The new organoids containing ER⁺ cells correctly showed no response to treatment with paclitaxel (Fig. 3d and e). The new organoids also correctly predicted the response of ER- cells to paclitaxel, demonstrating that cell viability is decreased when concentration of Paclitaxel was increased. However, conventional organoids predicted again erroneously the same response for MCF7 and MDA-MB-231 cells to paclitaxel (Fig. 3i and j). Hence, in this limited yet important test of drug response, our new organoids succeeded, while conventional organoids failed to predict clinical results.

Another important pre-clinical application of our method is to enable the study of tumor cells directly harvested from patients for screening of potential compounds or anti-cancer drugs. Our system can incorporate primary tumor cells with high efficiency (Supplementary Fig. 3a). These tumor organoids have a high success rate in comparison to conventional methods, which are not always capable of supporting primary tumor cell growth. Our system reproducibly establishes tumor cell growth from tumor tissues. Similarly to conventional organoid culture models, the growth of cells in these novel tumor organoids and subsequent invasion and migration into the outer collagen layer can be subjected to imaging modalities, allowing for the extraction of various quantifiable parameters, including confocal microscopy as well as sectioning and H&E staining of fixed samples (Supplementary Fig. 3b,c).

To further study the progression of cancer cells in our novel two-compartment model, we conducted live/dead assay staining of MDA-MB-231 organoids on day 1 and day 7. From the fluorescent images, we observed that cells began to proliferate and organize in small clusters, as seen in traditional Matrigel-only organoid cultures (Supplementary Fig. 3d). By day 7, there was evidence of cell death in the core of the organoid, which is also observed in hypoxic human patient tumors: a necrotic core developed as tumor cells expanded (Supplementary Fig. 3d) [46,47].

Next, we demonstrated the ability to co-culture two types of cells in the two compartments of our organoids. Cancer cells were embedded in the inner Matrigel core, while the outer collagen layer was impregnated with immune cells. This co-culture mimics the situation where the presence of cancer cells in a tissue induces an immune response mediated by the infiltration of immune cells from neighboring blood vessels into the stromal matrix. We confirmed our ability to encapsulate primary human monocytes and U937 human macrophages in the outer collagen layer and to monitor their influence on the growth and invasion of cancer cells via live-cell phase-contrast microscopy (Supplementary Fig. 3e,f). Based on MDA-MB-231-mCherry labeled cells

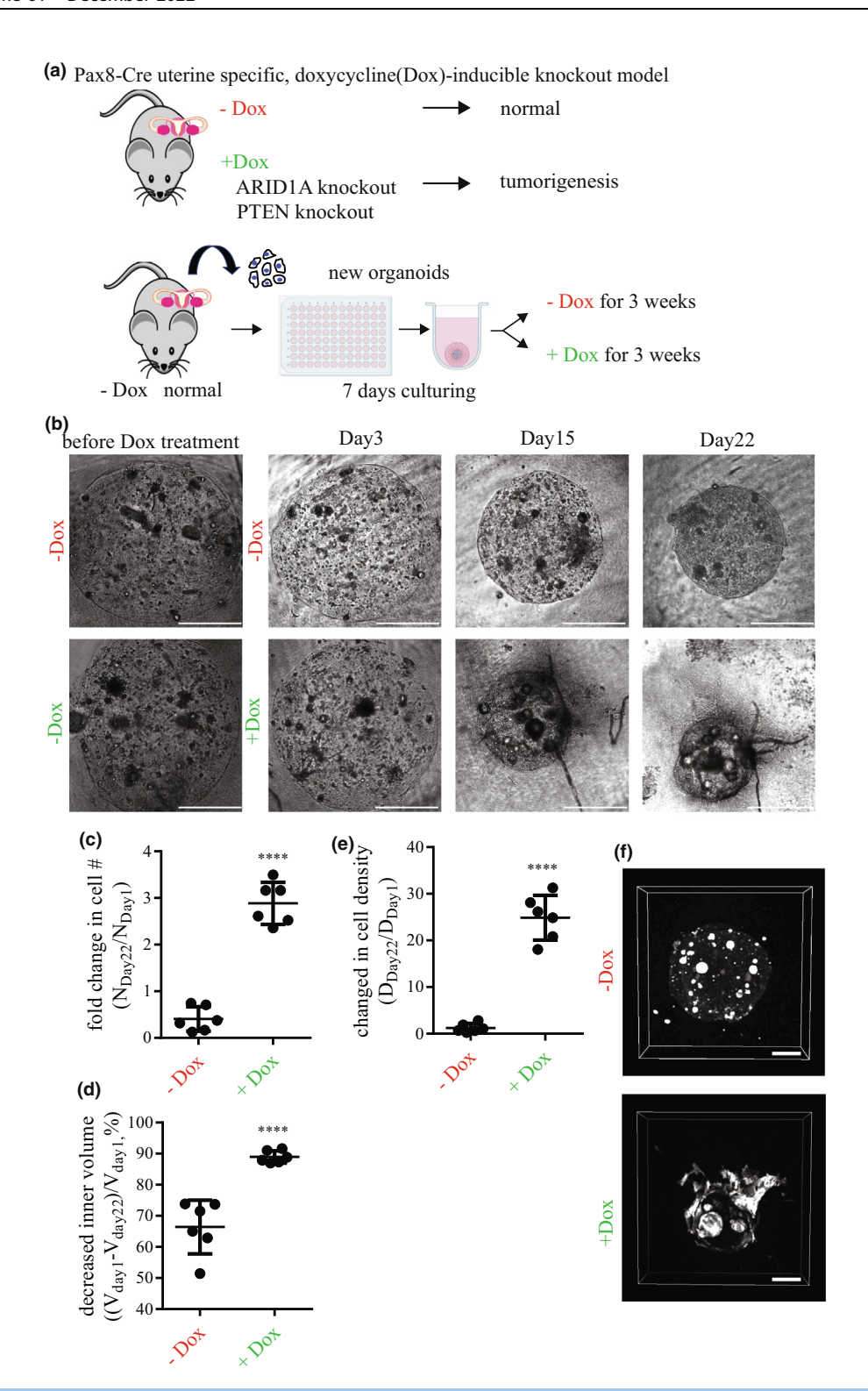
and U937-GFP cells, we were able to visualize immune-cancer cell interactions in our system (Supplementary Fig. 3g). In future work, we will use this new co-culture system to study the molecular mechanisms by which immune microenvironment affects tumor phenotypes and vice versa [40].

Validation of the new organoids in vivo

Next, we compared the progression of the new organoids in vitro and in vivo in three different cancer models. In the first cancer model, we compared the progression of primary uterine cells isolated from the doxycycline-inducible ARID1a and PTEN conditioned knockout mice in our two-compartment matrix to the progression of the cells in orthotopically implanted tumors in mice (Fig. 4a). ARID1A and PTEN are two key tumor suppressors in endometrioid carcinoma, the most common type of human uterine carcinoma and ARID1A mutation and loss of its expression correlate with tumor invasion in human endometrial carcinoma [48–52]. Deletion of ARID1A significantly accelerates tumor progression of PTEN -deleted endometrial and ovarian carcinomas as evidenced by marked invasion and metastasis in genetically engineered mouse models [53,54]. The knock-out is verified via IHC of both doxycycline-treated and control uterine cells. We utilized this knock-out inducible cell line to demonstrate the ability of our system to mimic in vivo observations.

First, we isolated the epithelial cells from the mouse uterus and cultured them in our organoid model. As anticipated, untreated cells formed regular structures in the inner Matrigel compartment (Fig. 4b). After doxycycline treatment to delete ARID1A and PTEN, cells started to propagate, as anticipated due to the increase in invasion of cancer in the mouse model (Fig. 4c); the volume of the inner Matrigel sphere was reduced more rapidly (due to cell contractility) in treated cells compared to untreated ones (Fig. 4d). Accordingly, cell density was 20-fold higher in the doxycycline-treated organoids than untreated ones (Fig. 4e). Importantly, we observed cell invasion into the surrounding collagen matrix (Fig. 4f). A similar pattern of tumor progression was seen in mice which showed endometrioid carcinomas two weeks after ARID1A / PTEN co-deletion by doxycycline treatment [53]. These carcinoma cells were highly invasive, with individual tumor cells infiltrating through uterine myometrium and permeating angiolymphatic spaces. In contrast, tumor formation was not observed in the absence of doxycycline administration (Supplementary Fig. 4a-d).

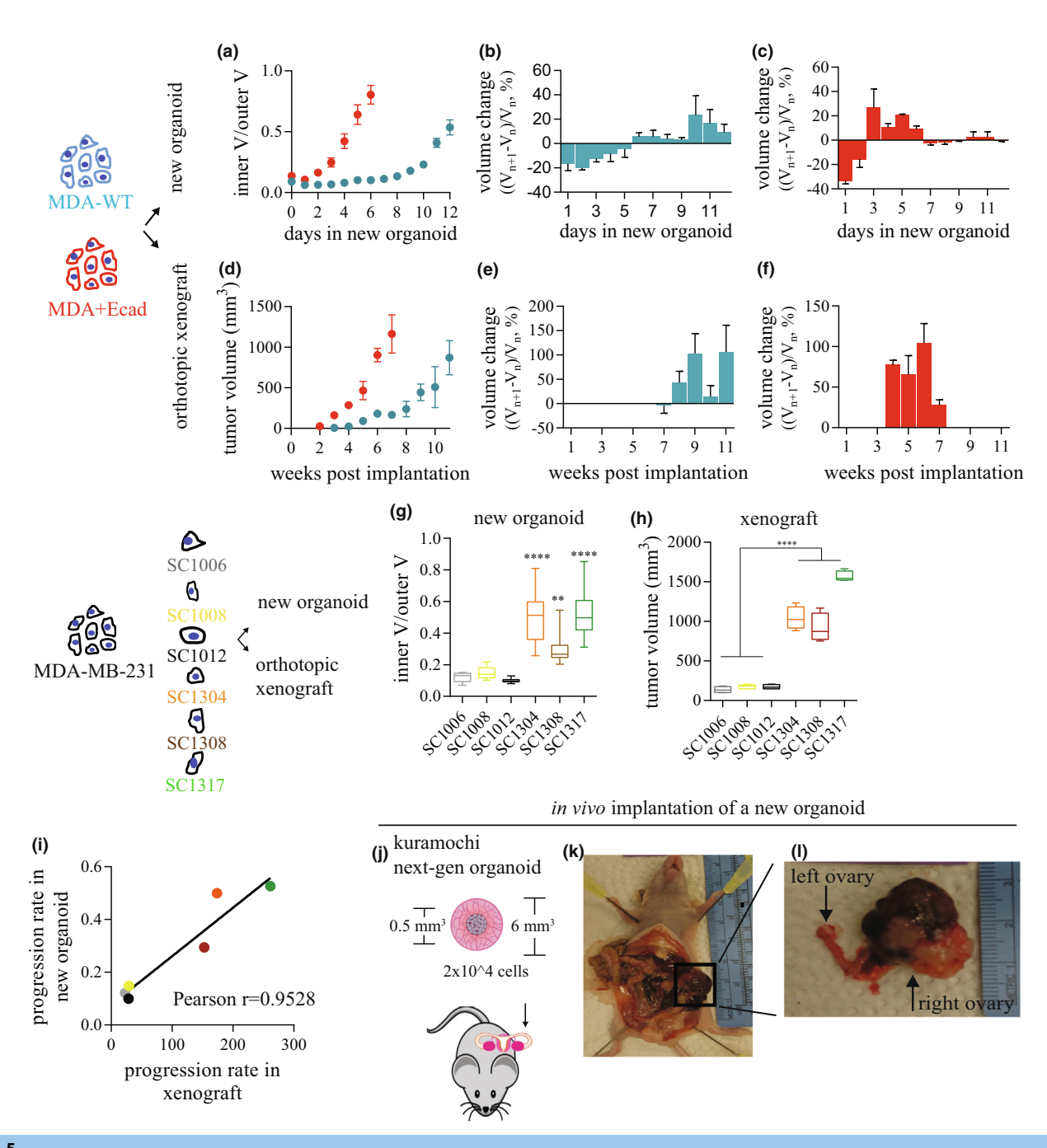
In a second model, we assessed the predictive power of our organoids of outcomes *in vivo* by examining the effect of E-cadherin on tumor progression. High expression of E-cadherin is associated with the poor overall survival of patients diagnosed with breast cancer (Supplementary Fig. 4e) [55,56]. To examine this scenario *in vitro*, we chose MDA-MB-231 cells, a commonly used TNBC type cell line that does not express E-cadherin. We employed a gain-of-function approach by generating an E-cadherin lentiviral knock-in of MDA-MB-231 cells, termed here MDA + Ecad cells (Supplementary Fig. 4f) [57]. In our organoids, before reaching the same tumor size, the progression rate of MDA + Ecad tumors was twice as high as control MDA-MB-231 tumors (Fig. 5a). After two days, MDA + Ecad tumors entered a growth phase, while it took nine days for control MDA-MB-231 tumors to reach a growth phase (Fig. 5b and c). When cells were



Two-compartment organoids mimic tumor progression *in vivo*. (a) Schematic of two-compartment organoids containing primary cancer cells harvested from tumors that formed in doxycycline-inducible Arid1a and Pten knockout mice. (b) Phase-contrast images of two-compartment organoids made of a Matrigel core containing the cancer cells and an outer collagen I compartment surrounding the core, in the absence and the presence of doxycycline. There is a significant increase in (c) cell number (d) volume shrinkage of the inner Matrigel sphere (e) cell density after doxycycline treatment. (f) Confocal images of new organoids in which the cells were labeled with F-actin. Scale bar, 200 µm. All two-compartment organoids had a Matrigel core and Collagen I as the outer compartment.

orthotopically implanted in the mammary fat pad of female NOD/SCID mice, their growth in the xenograft model correlated closely with our *in vitro* results using the new organoids:

MDA + Ecad tumors displayed a two-fold faster growth than MDA-MB-231 tumors (Fig. 5d). Within five weeks, the MDA + Ecad tumors reached a size of 1 cm³, while it took



Tumor growth in two-compartment organoids correlates with tumor growth *in vivo*. Tumor growth in (a) the two-compartment organoids *in vitro* or (d) the mouse mammary fat pad *in vivo*. Growth patterns of (b and e) MDA-MB-231 scramble control breast cancer cells (MDA-WT) and (c and f) MDA-MB-231 cells expressing E-cadherin (MDA + Ecad) in (b and c) the two-compartment organoids and (e and f) in the mouse mammary fat pad of NOD/SCID mice. The bar graphs represent the mean ± SEM of the tumor volume of organoids containing different single-cell clones selected from parental MDA-MB-231 cells. These different single-cell clone cells were either (g) incorporated in the two-compartment organoid or (h) implanted into the mouse mammary fat pad. (i) Correlation between tumor progression in the new organoids and in orthotopic xenograft mice. (j) Orthotopic implantation of two-compartment organoids into the ovary in the female nude mice. These organoids contain high-grade serous ovarian cancer Kuramochi cells in their core. (k) Tumor formation inside the abdominal cavity. (l) Tumor formation in ovaries. All organoids used in Fig. 5 were composed of a Matrigel core containing the cancer cells and an outer collagen I compartment surrounding the core. The following numbers of measurements were conducted: five biological repeats and six replicates per experiment (panels a–c); two biological repeats and five replicates per repeat (panel f), and two biological repeats and four replicates per repeat (panel h).

10 weeks for MDA-MB-231 tumors to reach the same size. MDA + Ecad tumors showed a significantly shorter lag phase comparing to the control MDA-MB-231 tumors (Fig. 5 e and f), all results predicted by the new organoids.

To further confirm the correlation between *in vivo* outcomes and outcomes predicted by modeling using the new organoids, we next selected six single-cell clones (SCs) generated from the parental MDA-MB-231 cell line and subjected them to both mod-

eling using new organoids and modeling using orthotopic xenografts *in* vivo. We correctly found that a subset of these clones displayed an aggressive growth, while a subset showed a low growth rate, both in the new organoids and in mice (Fig. 5g–i; Pearson coefficient of tumor growth rates in two-compartment organoids and mice was 0.95).

Finally, our new organoid culture can be used to generate orthotropic xenograft models. We implanted our twocompartment organoids containing high-grade serous ovarian cancer Kuramochi cells into the ovary of female nude mice (Fig. 5j). We chose this cell line because it is known to be nontumorigenic and challenging - if not impossible - to grow in nude mice [58-60]. Using our two-compartment matrix as vehicle, Kuramochi cells grew and formed tumors in the implanted ovary (Fig. 5i). We did not observe tumors that randomly grew on other organs in the abdomen (Fig. 5k), indicating that using our new organoid to deliver the cancer cells can greatly facilitate their implantation and growth only on target organs, whereas Kuramochi cells have only had limited success as an intraperitoneal injection [58]. Our novel methodology for organoid formation will greatly increase the clinical translatability of both in vitro and in vivo results.

Conclusion

We have developed a novel method to produce threedimensional bi-layered tumor organoids that allows for high levels of consistency, control, and correlation to *in vivo* models of cancer cells, all while being high throughput. In addition to improving from traditional organoid culture techniques, our technique is also a translational system that can be used to study cancers *in vivo* that do not have well-established or feasible models for *in vivo* study.

We show that by utilizing oil-in-water droplet microtechnology, we can conveniently generate two-compartment organoids that better mimic the tumor microenvironment than more traditional single-ECM organoids. We have also demonstrated through various control experiments how vital the presence of both reconstituted basement membrane and collagen layering is to generate a 3D in vitro model that closely correlates with in vivo data. The double-layered system allows for phenotyping and studying of cancer cell proliferation, invasion, and migration all in one experimental system and can be used to study cancers that are notoriously difficult to culture in the traditional 3D organoid systems, such as ovarian cancer. The novel technique we have developed allows for unmatched control of vital parameters to understanding how cancer cells proliferate and interact with the tumor microenvironment. The advantages of this system are extended to in vivo study of aggressive cancer types that lack well-established in vivo models. This approach will allow for further study of these cancers in pre-clinical mouse models to further improve patient outcome in the clinical setting. This platform will also allow for high-throughput drug screening, phenotyping, and predictive data acquisition that will greatly improve the too common disconnect observed between preclinical cancer research and clinical patient outcomes.

Methods

Cell culture of immortalized cell lines and genetic manipulations

MCF7 and MDA-MB-231 cells were cultured following ATCC guidelines in DMEM (Corning) with 10% FBS (Corning). For modified MDA-MB-231 cells, E-cadherin was artificially expressed via lentiviral knock-in, as described previously [55].

Two-compartment organoids made using oil-in-water droplet microtechnology

First mineral oil columns were generated utilizing unfiltered 10 μl pipette tips (USA Scientific) by creating a medium plug in the bottom of the tip with normal growth medium (i.e. DMEM with 10% FBS) prior to pipetting approximately 85 µl of mineral oil (Sigma) to the top of the pipette tip. Unless otherwise specified, the inner cores of our novel two-compartment organoid were made by mixing a determined number of cancer cells with 100 µl Matrigel (final concentration of 3 mg/mL) (Corning, Bedford, MA, USA). 1 μl of the mixture was pipetted into mineral oil column and incubated at 37 °C for 30 min to allow for the gelation of Matrigel. The Matrigel sphere containing the cancer cells was harvested from the mineral oil and rinsed $2\times$ with warmed serum-free medium. The cores were then resuspended in a type I collagen solution at a concentration of 2 mg/mL (Corning). 10 µl of the collagen mixture with one core was then pipetted into mineral oil column. The two-compartment sphere was incubated at 37 °C for 1 hour to allow for the gelation of type I collagen. The double-layered sphere was then collected and rinsed $2\times$ in warmed serum-free medium to remove all mineral oil prior to plating. Each new organoid was cultured in suspension in a round-bottom well. In Fig. 2, we modulate the matrices used in the core and outer compartments to demonstrate the effect of organoid architecture on the drug responsiveness of cancer cells.

Potential issues that may lead to unusable organoids: bubbles in Matrigel cores (which are lost in wash steps), picking up more than one core when adding the collagen layer, bubbles in collagen layer (will are lost during wash steps), and failure to completely remove the mineral oil (cores will pop-out of second layer).

For co-culture organoids, primary monocytes isolated from PBMCs or immortalized macrophage U87 cells were mixed into the collagen solution prior to the addition of the Matrigel cores containing MDA-MB-231 breast cancer cells to ensure homogenous solution of immune cells in collagen. For PMBC monocyte isolation, Human CD14⁺⁺CD16⁻ classical monocytes were isolated using Classical Monocyte Isolation Kit (Miltenyi Biotec) via negative selection. Briefly, PBMCs thawed from 90% HI-FBS/10% DMSO freezing medium were first blocked and labeled, followed by magnetic separation where label-free classical monocytes remained in the flow-through while non-monocytes were depleted.

Sample collection and tissue dissociation

Patients' tumor samples were acquired under Johns Hopkins Medicine Institutional Review Board approval (IRB00164685). Fresh tumor tissues were kept in the tissue storage medium (Miltenyi Biotech) and then processed using the tumor dissociation kit (Miltenyi Biotech) and gentleMACS Octo Dissociator with Heaters (Miltenyi Biotech) according to the manufacturer's instructions. Dissociated cells were washed in DPBS and directly seeded into the new organoids.

Time-lapsed and immunofluorescence microscopy

Time-lapsed images were collected every day for 1 week using a Nikon TE2000 microscope (Nikon) equipped with a $4\times$ objective and a Cascade 1 K CCD camera (Roper Scientific). The images were automatically stitched using custom MATLAB software (The MathWorks).

For fluorescence staining, organoids were fixed with 4% paraformal dehyde for 1 day and then incubated with the phalloidin (1:40; Invitrogen) and Hoe chst 33342 (1:100; Invitrogen) for 1 day at 4 °C. For tissue clearing, the commercial kit (Visikol) was used according to the manufacturer's instructions. Images of the stained cells were acquired with a Nikon A1 confocal microscope (Nikon) equipped with a 10× objective (Supplementary Fig. 5b–e). The 3D images were reconstituted using NIS-Elements (Nikon). For live-dead staining, cells were incubated with 2 μ M calcein-AM and 3 μ M propidium iodide for 4 h. Following incubation, organoids were imaged live with a Nikon A1 confocal microscope using a 10× objective.

Immune cell co-culture organoids were imaged on Ti2 (Nikon) using a $4\times$ PhL objective. Fluorescent images of m-Cherry tagged MDA-MB-231 breast cancer cells and GFP tagged U87 macrophages were taken on Nikon A1 confocal microscope with a $10\times$ objective.

For immunostaining for ZO-1 and E-cadherin, organoids were fixed with 4% paraformaldehyde for 1 day at 4 °C. To prepare to immunostaining, organoids were permeabilized with 0.5% Triton-X for 1 h and then blocked with 1% normal goat serum for 3 h. Organoids are then incubated with primary antibodies overnight at 4 °C. To prepare for imaging, organoids are washed in PBS prior to adding secondary antibodies, Hoechst, and phalloidin for 3 h in 1% normal goat serum. If necessary, organoids were subjected to tissue clearing with 60% glycerol, 2.5 M fructose solution for 20 min at RT. Organoids were imaged on Nikon AX confocal microscope with a 20× water immersion objective.

Drug response and cell viability

To examine the drug response of cancer cells, two-compartment organoids were manufactured, harvested and distributed in the wells of a 96-round-bottom plate. Each well contained a single organoid in 100 µl medium. Two times concentrated drug solution including tamoxifen (Sigma-Aldrich), paclitaxel (Selleckchem) as well as DMSO control 100 µl was added to each well. Cell viability was assayed using the cell viability reagent PrestoBlue (Thermo Fisher Scientific). The samples were incubated with PrestoBlue for 3 h. The fluorescence intensity of PrestoBlue was accessed using a Spectra Max plate reader (Molecular Device), according to the manufacturer's instructions. Standard curves relating the controlled initial number of seeded cells in the organoids to the measured PrestoBlue fluorescence intensity was generated before data analysis (Supplementary Fig. 5a). To confirm PrestoBlue assay as means to measure proliferation (i.e. increase in cell number), 10 organoids were lysed with 75 µl of high concentration SDS lysis buffer, needle sonicated for 10-15 pulses, and then heated at $100~^{\circ}\text{C}$ for 5 min to extract protein. MicroBCA kit (ThermoFisher) was used to conduct protein concentration assay and samples were measured on SpectraMax plate reader (Molecular Devices).

Volume and size tracking of two-compartment organoids

To track size of the two-compartment organoids, NIS-elements software was used to manually measure the individual compartments of organoids from phase contrast images taken with a 4x objective on TE2000 or Ti2 microscopes (Nikon).

Histology and immunohistochemistry

All organoids were fixed with 10% formalin for 24 h and then processed by The Johns Hopkins University Oncology Tissue Services using a standard paraffin tissue embedding protocol and 4- μm sections were cut. For immunohistochemistry, formalin fixed paraffin-embedded sections were deparaffinized and rehydrated. Antigen retrieval was carried out using DAKO Target Retrieval Solution, equivalent to citrate buffer pH 6.0, or Trilogy, equivalent to neutral pH EDTA. Endogenous peroxidase activity was quenched in 3% H_2O_2 . Sections were incubated with antibodies overnight at 4 °C. Immunostains were visualized using DAKO EnVision+ System-HRP goat Anti-Rabbit IgG and DAKO DAB+ Substrate Chromogen System. Nuclei were visualized using hematoxylin counterstaining. Cover slides were mounted with Cytoseal 60.

To merge the images of two slides from the adjacent sections, we developed a customized MATLAB software. The nucleus-isolated images were rigidly registered in order to computationally align the cells in adjacent sections. Once aligned, the same registration method was applied to the antibody stain-isolated channels of the IHC images.

Animals

All animal studies were in accordance with animal protocols approved by the Johns Hopkins Medical Institute Animal Care and Use Committee. Generation of Arid1aflox/flox mice on the C57BL/6 background was described previously [48]. Briefly, Ptenflox/flox mice on the BALB/c background (Strain C; 129S4-Ptentm1Hwu/J) were purchased from the Jackson Laboratory (Groszer et al., 2001). To express Cre recombinase specifically in the mouse uterine epithelium, we used Pax8-Cre mice which were generated by crossing mice expressing the reverse tetracycline-controlled transactivator (rtTA) under the control of the Pax8 promoter (Pax8-rtTA) with mice expressing Cre recombinase in a tetracycline-dependent manner (TetO-Cre). A knockout was initiated by treating mice with doxycycline either through oral gavage (2 mg/mouse/day) or subcutaneous implantation of doxycycline pellets (200 mg) when they reached puberty (6-8 week old).

Orthotopic mammary fat pad injection

A detail procedure is provided elsewhere [61]. Briefly, 5- to 7-week-old female NOD/SCID mice were used. Mice were anesthetized and 1×10^6 cells mixed with 100 ml Matrigel (Corning) were injected into the mammary fat pad (MFP). Tumors were

measured in three dimensions (a, b, and c), and their volume (V) was calculated as $V = abc \times 0.52$.

Orthotopic implantation of two-compartment organoids

Five- to 7-week-old female NOD/SCID mice were used. Once a mouse was an esthetized, we made an incision (7 mm) at the left back of the mouse to open the abdomen. The left ovary of the mouse was pulled out from the abdomen. We cut the surface of ovary and implanted a new organoid. Twenty μ l of Matrigel was applied to secure the placement of new organoid on the ovary. After the implantation, we released the left ovary and let it back to the abdominal cavity. We closed the peritoneum by suture and closed skin incision using a stapler.

CRediT authorship contribution statement

Meng-Horng Lee: Conceptualization, Methodology, Formal analysis, Investigation, Data curation, Writing - original draft, Visualization, Supervision, Project administration. Gabriella C. Russo: Conceptualization, Validation, Formal analysis, Investigation, Data curation, Writing - review & editing, Visualization, Supervision. Yohan Survo Rahmanto: Data curation, Formal analysis, Investigation, Methodology. Wenxuan Du: Validation, Formal analysis, Investigation, Data curation, Visualization. Ashleigh J. Crawford: Validation, Formal analysis, Investigation, Data curation, Visualization. Pei-Hsun Wu: Funding acquisition, Formal analysis, Software, Visualization, Supervision. Daniele Gilkes: Investigation, Data curation, Methodology. Ashley Kiemen: Formal analysis, Visualization, Software. Tsutomu Miyamoto: Data curation, Formal analysis, Investigation, Methodology. Yu Yu: Data curation, Formal analysis, Investigation, Methodology. Mehran Habibi: Investigation, Resources. Ie-Ming Shih: Resources, Supervision, Writing - review & editing, Methodology, Supervision. Tian-Li Wang: Resources, Supervision, Writing – review & editing, Methodology, Supervision. Denis Wirtz: Conceptualization, Methodology, Writing – original draft, Writing – review & editing, Supervision, Funding acquisition, Resources, Project administration.

Declaration of Competing Interest

The authors declare that they have no known competing financial interests or personal relationships that could have appeared to influence the work reported in this paper.

Acknowledgements

We thank all members of the Wirtz Lab for discussions and feedback on this project. This work was supported through grants from the National Cancer Institute (U54CA143868 and U54CA268083) and the National Institute on Aging (U01AG060903) to D.W. and P.H.W.

Contributions

M.H.L. and D.W. developed the hypothesis and designed experiments. M.H.L., G.C.R., D.G., W.D., and A.J.C. performed experiments and data analysis. Y.S.R., T.M., Y.Y., T.L.W., and I.M.S. performed *in vivo* validation experiments and implanted orga-

noids into mice for *in vivo* studies. M.H. prepared breast tumors from patients for primary cell experiments. A.K. and P.W. performed image analysis. M.H.L., G.C.R. and D.W. wrote the manuscript with input from P.W., I.M.S., T.M., and T.L.W.

Appendix A. Supplementary data

Supplementary data to this article can be found online at https://doi.org/10.1016/j.mattod.2022.07.006.

References

- [1] N. Sachs et al., Cell 172 (2018) 373-386.e10.
- [2] S.F. Boj et al., Cell 160 (2015) 324-338.
- [3] M. van de Wetering et al., Cell 161 (2015) 933-945.
- [4] M.Y. Turco et al., Nat. Cell Biol. 19 (2017).
- [5] L. Broutier, et al. Human Primary Liver Cancer–derived Organoid Cultures for Disease Modeling and Drug Screening. *Nature Publishing Group* (2017) doi:10.1038/nm.4438.
- [6] D. Gao et al., Cell 159 (2014) 176-187.
- [7] G. Vlachogiannis, et al. Patient-Derived Organoids Model Treatment Response of Metastatic Gastrointestinal Cancers. https://www.science.org.
- [8] S.H. Lee et al., Cell 173 (2018) 515-528.e17.
- [9] N. Lugli et al., Cell Rep. 19 (2017).
- [10] J. Drost, H. Clevers, Nat. Rev. Cancer 18 (2018) 407-418.
- [11] X. Li et al., Nat. Med. (2014), https://doi.org/10.1038/nm.3585.
- [12] L.D. Nadauld et al., Genome Biol 15 (2014) 428.
- [13] L.E. Dow et al., Cell 161 (2015) 1539-1552.
- [14] E. de Sousa, F. Melo, et al., Nature 543 (2017) 676-680.
- [15] K.P. O'Rourke et al., Nat. Biotechnol. 35 (2017).
- [16] J. Roper et al., Nat. Biotechnol. 35 (2017) 569-576.
- [17] B.-K. Koo, et al. 112 (2015).
- [18] A. Cristobal et al., Cell Rep. 18 (2017) 263–274.
- [19] K.J. Cheung et al., Cell 155 (2013) 1639–1651.
- [20] N. K. Finnberg, et al. Oncotarget 8 (2017) www.impactjournals.com/oncotarget/
- $[21]\ M.\ Crespo,\ et\ al.\ Nat.\ Med.\ 23\ (2017)\ 878–884.$
- [22] C.S. Verissimo et al., Elife 5 (2016).
- [23] A.C. Rios, H. Clevers, Nat. Methods 15 (2018) 24–26.
- [24] M. Huch et al., Development 144 (2017) 938–941.
- [25] B. Phipson et al., Nat. Methods 16 (2019) 79–87.
- [26] F. Weeber, et al. The Netherlands; c Cancer Genomics.nl, 3584 CG Utrecht, The Netherlands; d Foundation Hubrecht Organoid Technology (HUB), 3584 CT. Academy of Arts and Sciences 3584.
- [27] N. Phan, et al. doi:10.1038/s42003-019-0305-x.
- [28] J.N. Beck et al., Biomaterials 34 (2013) 9486-9495
- [29] H. Jayatilaka et al., Oncotarget 9 (2018) 32556–32569.
- $[30]\,$ H. Jayatilaka, et al. Nat. Commun. 8 (2017)1–12.
- [31] A.M.J. Valencia et al., Oncotarget 6 (2015) 43438–43451.
- [32] P.-H. Wu et al., PNAS 111 (2014) 3949–3954.
- [33] J. Kondo, et al. doi:10.1073/pnas.1015938108.
- $[34]\ \ P.\ A.\ Kenny,\ et\ al.\ (2007)\ doi:10.1016/j.molonc.2007.02.004.$
- $[35] \ R. \ Kalluri, \ Nat. \ Rev. \ Cancer \ 3 \ (2003) \ 422–433.$
- [36] D. Wirtz, K. Konstantopoulos, P.C. Searson, (2011) doi:10.1038/nrc3080. www.nature.com/reviews/cancer.
- [37] M. J. Bissell, D. Radisky, Nat. Rev. Cancer 1 (2001) 46–54.
- $\hbox{[38] J. Chang, O. Chaudhuri, J. Cell Biol. 218 (2019) 2456–2469.}$
- [39] C. Marar, B. Starich, D. Wirtz, Nat. Immunol. 22 (2021) 560–570.
- [40] W. Du, et al. 24 (2022) https://doi.org/10.1146/annurev-bioeng-110320-110749.
- [41] S.P. Carey, K.E. Martin, C.A. Reinhart-King, Sci. Rep. 7 (2017).
- [42] S. Vukicevic et al., Exp. Cell Res. 202 (1992) 1-8.
- [43] M. Colleoni et al., Clin. Cancer Res. 10 (2004) 6622-6628.
- [44] R. Rouzier et al., Clin. Cancer Res. 11 (2005) 5678–5685.
- [45] O. Abe et al., The Lancet 378 (2011) 771-784.
- [46] D.M. Gilkes, G.L. Semenza, D. Wirtz, Nat. Rev. Cancer 14 (2014) 430–439.
- [47] I. Godet et al., Nat. Commun. 10 (2019) 1-18.
- [48] L. Li, et al. (2020) doi:10.1002/path.5566.
- [49] T.T. Yen et al., Gynecol. Oncol. 150 (2018) 426-431.
- [50] A. Ayhan, et al. doi:10.1002/cjp2.22.
- [51] T.L. Mao et al., Am. J. Surg. Pathol. 37 (2013) 1342.

- [52] A. Ayhan et al., Int. J. Gynecol. Cancer 22 (2012) 1310–1315.
- [53] Y. Suryo Rahmanto et al., Nat. Commun. 11 (2020) 1–14.
- [54] B. Guan et al., J. Natl. Cancer Inst. 106 (2014).
- [55] K. Chu, et al. Oncotarget. 4 (2013) www.impactjournals.com/oncotarget.
- [56] M. Ringnér et al., PLOS ONE 6 (2011) e17911.

- [57] M.H. Lee et al., Biophys. J. 102 (2012) 2731.
- [58] A.K. Mitra et al., Gynecol. Oncol. 138 (2015) 372–377.
- [59] A. de Haven Brandon et al., Sci. Rep. 10 (2020) 1–13.
- [60] K.M. Elias et al., Gynecol. Oncol. 139 (2015) 97–103.
- [61] J.A. Ju et al., Mol. Cancer Res. 15 (2017) 723–734.